Effect of optical comb profile in optically injected semiconductor lasers

NAJM M. AL-HOSINY*

Department of Physics, College of Science, Taif University, P.O. Box 1109, Taif 21944, Saudi Arabia

This study explores the nonlinear dynamics of semiconductor lasers under optical injection from diverse frequency comb profiles, including Gaussian, Lorentzian, graded, quadratic, and zigzag distributions. Using numerical simulations of injection-locking maps, bifurcation diagrams, and carrier dynamics, we analyze the stability and chaos within these systems. Results show that Gaussian and Lorentzian combs produce smooth and predictable locking regions, with heightened instability near chaotic thresholds. Graded combs ensure stable performance across varying injection conditions, whereas quadratic and zigzag combs exhibit fragmented yet stable locking boundaries. These findings provide insights for optimizing optical systems leveraging frequency combs for telecommunications and metrology.

(Received January 14, 2025; accepted August 5, 2025)

Keywords: Semiconductor lasers, Optical injection, Frequency comb, Chaos, Carrier density

1. Introduction

Injection locking in semiconductor lasers has been a cornerstone of nonlinear optical studies, with foundational works by Kobayashi and Kimura establishing key principles governing phase locking and amplitude stability in AlGaAs lasers under optical injection [1]. Mogensen et al. extended these principles by exploring the stability conditions and locking phenomena across a range of detuning and injection strengths, providing a framework that has underpinned many modern studies [2]. More recently, Liu and Slavík presented a comprehensive review linking these principles to contemporary applications, such as optical communications and frequency comb stabilization [3].

Frequency comb generation, a significant advancement in the field, has been widely investigated. Gain-switching methods enable precise control of pulsed comb generation in externally injected semiconductor lasers [4]. Dual-mode injection locking has been particularly effective in generating high-speed, stable combs suitable for telecommunications [5]. Tang and Hung advanced this approach by demonstrating cascaded injection techniques to enhance tunability and broaden application scope [6]. Similarly, Hussein et al. showcased the potential of passive frequency combs for compact and energy-efficient systems [7].

One of the main phenomena observed in optically injected semiconductor lasers is chaos. Chaos plays a crucial role in the nonlinear dynamics of optically injected lasers, providing opportunities for applications such as secure communications and high-resolution sensing. We have previously explored chaos tailoring in optically injected lasers [8], while Doumbia et al. examined wideband chaos induced by optical injection, linking it to the interplay between detuning and injection parameters [9-10]. Borodkin et al. demonstrated that noise injection could broaden comb frequencies, offering insights into managing spectral properties in chaotic regimes [11].

Several studies have delved into the effect of injection profiles on comb dynamics. For instance, Al Mulla [12] explored microwave comb generation through double-locked semiconductor lasers, highlighting the significance of phase control in achieving stable frequency spacing. Other Works [13-14] focused on phase modulation and noise suppression, underscoring the importance of stabilizing injection parameters to optimize comb performance. Zhang et al. extended this understanding by developing high-conversion-efficiency Kerr frequency combs, emphasizing the role of nonlinear optical interactions in improving performance [15].

Carrier dynamics in optically injected lasers have been extensively studied. In previous work, we linked changes in carrier density to frequency shifts, offering insights into the interaction between carrier populations and laser output stability [16]. Further work by Khan et al. examined dynamic shaping of combs in quantum cascade lasers [17], while Gavrielides focused on sideband suppression and spectral narrowing [18].

Techniques for stabilizing and expanding frequency combs have also been a focus. Moon et al. [19] used femtosecond laser injection locking to amplify specific

comb modes, and Rosado et al. [20] achieved pulsed combs via step-recovery diodes. Advances in harmonic frequency locking, demonstrated tunable comb spacing through optical injection, further enriching the design possibilities for frequency comb applications [21].

Recently, attention has shifted toward enhancing spectral purity and managing chaotic behavior. Ulanov et al. [22] and Wildi et al. [23] presented self-injection locking techniques for microcombs, achieving phase stabilization and improved spectral control. These methods complement broader studies on nonlinear dynamics in comb systems, such as those by Wieczorek et al. [24] and Stroganov et al. [25], which provide comprehensive frameworks for understanding chaos and multi-stability in optical systems.

Frequency combs also play a pivotal role in emerging technologies, such as terahertz generation and metrology. Sharma et al. [26] demonstrated four-wave mixing in highly nonlinear fibers to generate combs with tunable spacing, while Doumbia et al. [27] explored nonlinear laser dynamics under comb injection, revealing potential for chaos-assisted applications. Work by Li et al. [28] on attractor reconstruction for chaotic lasers highlights the versatility of combs in randomness evaluation and secure communication. We also studied the effects of frequency comb spacing on locking bandwidth and frequency shifts in semiconductor lasers [29]. The results highlight how comb spacing influences the locking region boundaries and induces frequency pushing and pulling. Recently, we have investigated frequency shifts in semiconductor lasers influenced by optical frequency comb injection [30]. Using numerical simulations, the study identifies frequency pushing and pulling phenomena, revealing their dependence on comb parameters such as spacing and line numbers. The dynamics are linked to carrier density variations, with practical implications for laser stabilization and telecommunication applications.

In this study, we aim to explore the nonlinear dynamic behavior of semiconductor lasers (SLs) under optical injection from a range of frequency comb profiles, including normal, Gaussian, Lorentzian, graded, quadratic, and zigzag distributions. By constructing injection locking maps, we will analyze the locking behaviors, intermittency, and chaotic dynamics as functions of detuning and injection levels. Our investigation will also evaluate how varying comb profiles and frequency spacing impact the stability and predictability of the locking regions. Through bifurcation diagrams and carrier dynamics analysis, we will uncover the stability advantages of graded and quadratic combs and the propensity of Gaussian and Lorentzian combs to transition into chaotic dynamics. While frequency comb generation is traditionally associated with multimode or mode-locked lasers, this study adopts a different approach: it investigates the nonlinear dynamics induced in a single-mode semiconductor laser when injected with frequency combs of varying spectral profiles. The motivation lies in the potential to use comb injection not for comb generation, but to modulate and control laser behavior, including locking bandwidth, spectral purity, and the onset of chaotic regimes. This may offer valuable tools for tailoring laser output characteristics in compact or constrained systems, where full comb generation is not feasible or necessary.

2. Materials and methods

The model used in our simulation builds upon Lange's approach [16] to investigate the dynamics of a semiconductor laser (SL) under the injection of various frequency comb profiles from a master laser (ML). The model is a basic injection locking model with a ML being injected into a SL. The ML is considered to produce six comb structures: normal, Gaussian, Lorentzian, graded, quadratic, and zigzag combs, as shown in Fig. 1, respectively. Each comb comprises five equally spaced signals, with the central signal serving as the main reference for detuning relative to the free-running SL frequency. This spacing is kept at 0.2 GHz in most of the study.

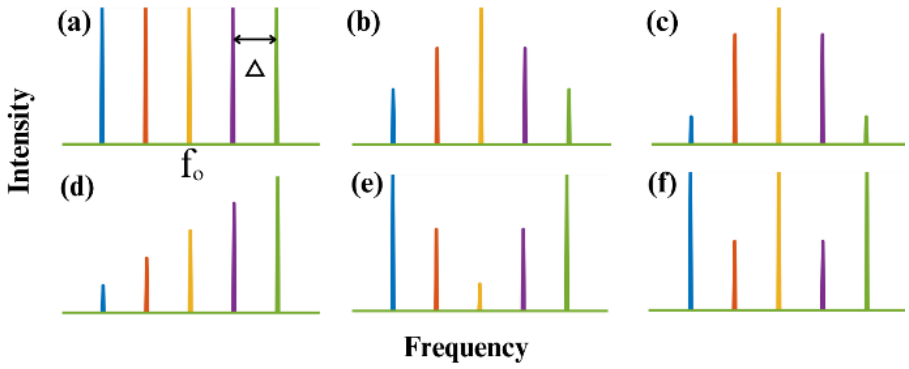

Fig. 1. Structure of the combs used in our study: (a) normal, (b) Gaussian, (c) Lorentzian, (d) graded, (e) quadratic and (f) zigzag comb. All combs consist of five signals that are equally spaced with Δ GHz, and the central signal is regarded as the main signal in terms of detuning (colour online)

The dynamics of the system are governed by the following rate equations, which describe the evolution of the electric field amplitude, phase, and carrier density [29]. The equation for the electric field amplitude is given by:

$$\frac{d}{dt}E_o(t)=\frac{1}{2}\ G_N\ \Delta N(t)\ E_o(t)+\eta\ \left[\sum E_m\ \cos(\Delta t_m)\right] \quad (1)$$

where $E_o(t)$ is the SL electric field, G_N is the differential gain coefficient, $\Delta N(t) = N - N_{th}$ is the population inversion with N as the carrier density and N_{th} as the threshold carrier density, η is the coupling coefficient, and $\Delta\phi_m=\Delta\omega_m t-\phi_o(t)$ is the phase difference between the SL and ML, with $\Delta\omega_m=\omega_m-\omega_o$. The equation for the phase dynamics is:

$$\frac{d}{dt}\phi_o(t)=\frac{1}{2}\ \alpha\ G_N\ \Delta N(t)\ +\eta\left[\sum\frac{E_m}{E_o(t)}\ \sin(\Delta t_m)\right] \quad (2)$$

where $\phi_o(t)$ is the SL phase and α is the linewidth enhancement factor LEF (Henry factor). Finally, the carrier density dynamics are described by:

$$\frac{d}{dt}N(t)=J-\frac{N(t)}{\tau_s}-G_N(N(t)-N_o)\ E_o^2(t) \quad (3)$$

where J is the injected current density, and τ_s is the carrier lifetime. The injection level K is defined as $K=E_m/E_o$, representing the ratio of the ML comb's electric field to that of the SL. In this model, the gain term $G_N \cdot \Delta N(t)$ uses a differential gain formulation, where G_N represents the differential material gain and implicitly includes the confinement factor Γ via calibration. This approach is valid for modeling dynamical behavior near threshold where gain saturation is negligible [16].

Numerical integration of these equations using the Runge-Kutta method allows the construction of injection locking maps, which detail the locking, chaotic, and intermittent dynamics as functions of detuning and injection level. The parameters used in our study are experimentally determined and listed in Table 1 [16].

Table 1. Parameters' values used in our simulation

Parameter	Symbol	Value
Wavelength	λ	1556.6 nm
Differential Gain	G_N	1.4×10^{-12} $m^3\ s^{-1}$
Carrier lifetime	τ_s	0.43 ns
Photon lifetime	τ_p	1.8 ps
Coupling rate	η	$9 \times 10^{10}\ s^{-1}$
Transparency carrier density	N_o	1.1×10^{24} m^{-3}
Threshold carrier density	N_{th}	1.5×10^{24} m^{-3}
Normalized injection current	I / I_{th}	2

Finally, the comparison between different frequency comb profiles in this study is established on several standardized criteria to ensure fairness and consistency. First, all comb profiles have equal bandwidth, as depicted in Fig. 1, ensuring a uniform spectral extent across the profiles. Second, the detuning is consistently referenced to the central signal frequency, maintaining an equivalent baseline for evaluating locking behavior and spectral dynamics. Lastly, the maximum power of the comb profiles is normalized to the same value, allowing for direct comparison of their effects on the dynamic response of the injected semiconductor laser without bias introduced by varying power levels.

3. Results and discussion

To examine the effect of comb type on the nonlinear dynamics of semiconductor lasers when subject to the injection of frequency comb, we draw the injection locking maps for the 6 types of combs. The injection locking map represents the dynamic behavior of the laser when subjected to an external optical injection. This map is typically plotted with the frequency detuning (Δf) on one axis and the injection strength (K) on the other axis. It helps in visualizing different operational regimes of the laser, such as injection locking, periodic oscillations, and chaotic behavior. In our case, we recorded the frequency shift of the free-running SL at each point of this map. In other words, if the frequency shift of the SL is equal to the ML, that means the SL is locked to the ML. Fig. 2 a shows a typical injection locking map of the SL, when subjected to the injection of

normal frequency comb (equal intensities of all signals). One can see that the SL is locked to the ML if the frequency shift of the free-dunning SL signal is equal to the injected ML frequency. In other words, the locking region is the area with a color gradient. Outside this region, the free-running SL experiences a pushing effect as will be discussed shortly. Fig. 2 shows 6 injection locking maps of the SL when injected by normal, Gaussian, Lorentzian, graded, quadratic and zigzag, respectively. All combs are with equal spacings of 0.2 GHz. A detailed inspection of the figure reveals that the normal comb exhibits well-defined locking regions, particularly in mid-range detuning and injection levels, reflecting a predictable interaction between the equally spaced modes of the comb and the laser. Both the Gaussian and Lorentzian combs show similar behavior, as they concentrate power around the central frequency with a tapering effect toward the side modes. This results in relatively narrow locking regions, with the Gaussian comb providing smoother transitions due to its more gradual power decay, while the Lorentzian comb's sharper power drop-off introduces slightly more spread and nonlinearities in the locking map. However, both combs are effective in producing predictable locking especially around the central frequencies. The graded comb presents a continuous and smooth locking region, thanks to its gradual power reduction, leading to more stable behavior at lower injection levels. On the other hand, the quadratic comb demonstrates fragmented and irregular locking regions, as the uneven power distribution makes the laser highly sensitive to the injected frequencies. Finally, the zigzag comb shows fewer locking regions, as the alternating power levels destabilize the laser's locking ability, particularly at higher injection levels. Overall, combs with concentrated power distributions, like the Gaussian and Lorentzian types, yield more predictable and narrow locking regions, while those with uneven power distributions, such as the quadratic and zigzag combs, lead to more fragmented and complex dynamics.

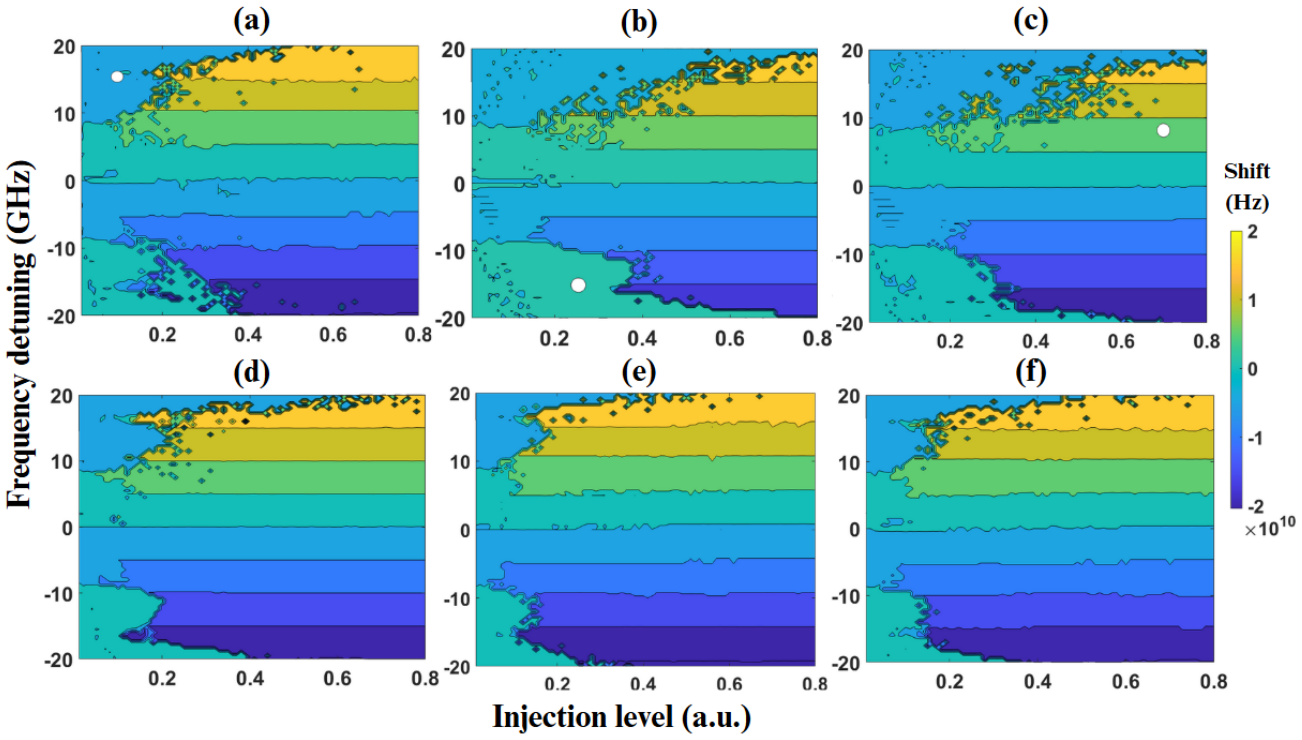

Fig. 2. Injection locking maps of the SL under the injection of: (a) normal, (b) Gaussian, (c) Lorentzian, (d) graded, (e) quadratic and (f) zigzag comb. The spacing in this case is 0.2 GHz and the color bar in the right illustrates the shift in the free-running SL peak. The white circles in (a), (b) and (c) represent the operating points at which the spectra in Fig. 3 are taken, respectively (colour online)

Another observation that can be seen in the map is the intermittency (dots) at the boundaries of the locking region, more obviously, at the upper boundary. This intermittency indicates regions of partial locking, where the semiconductor laser momentarily locks to the injected signal but intermittently breaks free due to nonlinear effects. This is typically seen in regions of higher frequency detuning and injection strength, where the laser is on the edge of chaotic behavior. In this aspect, the six injection locking maps reveal varying degrees of intermittency at the upper boundary of the locking regions for each comb type. The normal comb shows a moderate amount of intermittency, with some scattered dots indicating transitions between locking and unlocking behavior. The Gaussian comb exhibits slightly more intermittency, with a more pronounced presence of dots at the upper boundary,

suggesting increased instability as detuning increases. The Lorentzian comb exhibits the highest level of intermittency, with numerous scattered dots along the upper boundary, indicating significant instability due to the sharper power distribution decay. The graded comb, however, shows moderate intermittency, placing it in the middle in terms of instability, with more dots than the quadratic or zigzag combs, but less chaotic than the Lorentzian and Gaussian combs. Interestingly, the quadratic and zigzag combs show the least intermittency, with very few dots at the upper boundary, suggesting that despite their uneven or alternating power distributions, these combs produce smooth locking regions with fewer transitions between locking and non-locking states. This analysis reveals that the Lorentzian comb induces the most instability, while the quadratic and zigzag combs surprisingly result in the most stable boundaries.

To reconcile both findings, we conclude that Gaussian and Lorentzian combs, with their smoothly tapering power distributions, provide more predictable and continuous locking regions overall, resulting in smoother transitions between locked and unlocked states across the injection map. In contrast, quadratic and zigzag combs, with their uneven power distributions, produce more fragmented and complex locking dynamics, meaning the overall locking regions are more irregular and less predictable. However, when examining intermittency at the upper boundary, we observe that the quadratic and zigzag combs exhibit less intermittency (fewer dots), indicating greater stability near the boundary compared to the Lorentzian and Gaussian combs. This suggests that while quadratic and zigzag combs may have more fragmented locking patterns throughout the map, they show fewer unstable transitions near the upper boundary. In summary, Gaussian and Lorentzian combs provide smoother, more predictable locking behavior overall, while quadratic and zigzag combs, despite their irregularity, demonstrate more stability at the upper detuning boundary.

Let us now see the typical dynamics shown in the map. Fig. 3 shows three spectra taken at the marks shown in Fig. 2 a, b and c, respectively. Fig. 3 a illustrates the spectrum of the system when a normal comb is injected at a detuning of +15 GHz and an injection level of 0.1. We can see that the free-running SL is not locked to the ML comb at 15 GHz and is slightly affected by this injection. This effect is appearing in the minor frequency shift as shown in the inset of the figure. The SL peak is slightly shifted towards the negative detuning side (redshift). As the ML comb is injected in the positive detuning side and the SL is shifted away, this phenomenon is called frequency pushing and is attributed to the carrier density dynamics [16]. This phenomenon is observed outside the locking region and away from the locking boundaries, even when the ML comb is injected in the negative detuning side as shown in Fig. 3 b. In this figure, the SL main peak (highest signal) is shifted towards the positive detuning side as the ML comb is injected at -15 GHz, regardless of the injection level (which is in this case around 0.25). Finally, the behavior shown in Fig. 3 c is a typical injection locking dynamic as the SL is locked to the ML comb at +8 GHz and injection level of 0.7. Note that this locking is not a stable locking as the side peaks are strongly presented in the cavity. Note that, in this study, the term locking refers to the condition where the slave laser (SL) frequency follows that of the master laser (ML). However, this does not imply stable locking in the strict spectral sense, which typically requires > 30 dB suppression of side modes. Due to the relatively high injected comb power, such suppression is not observed in our simulations, and the locking behavior shown in Figs. 2 and 4 should be interpreted as unstable locking.

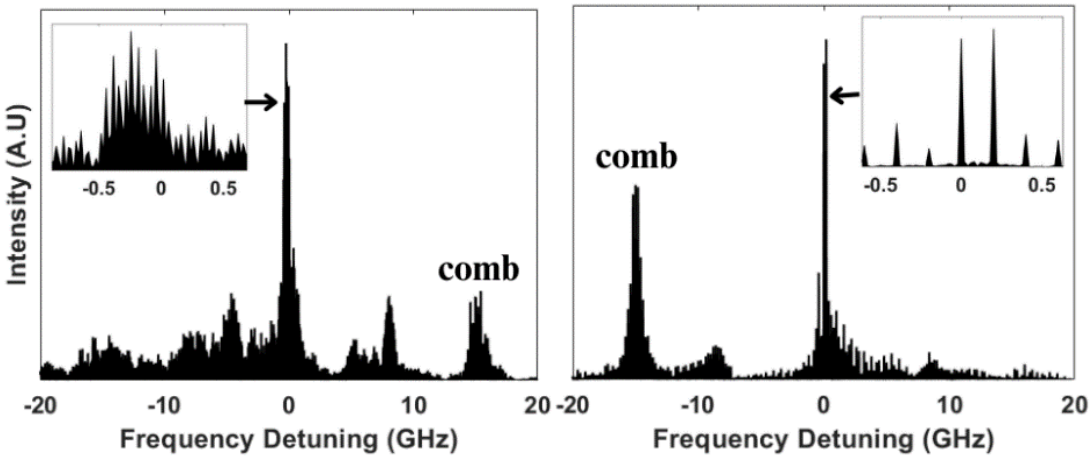

(a) *(b)*

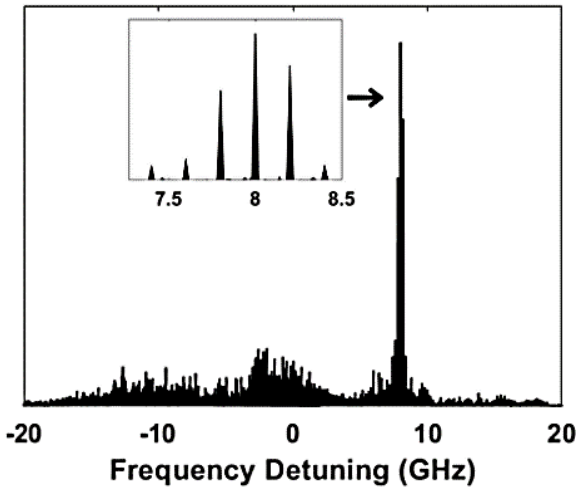

(c)

Fig. 3. Optical spectra of the injected SL (linear scale) at the points shown in Fig. 2 a, b and c, respectively. The insets are magnification of the main peaks

We regenerate the six maps of the different frequency combs but this time at a spacing of 0.8 GHz. Such maps are shown in Fig. 4. When comparing Fig. 4 to Fig. 2, we observe significant differences in the injection locking characteristics of the slave laser (SL) under various frequency comb injections. This contrast is largely due to the change in frequency spacing of the injected signals, which has increased from 0.2 GHz in Fig. 2 to 0.8 GHz in Fig. 4. This alteration in spacing has a marked impact on the stability and breadth of the locking regions across different comb types, revealing how frequency spacing affects the dynamic response of the SL under optical injection.

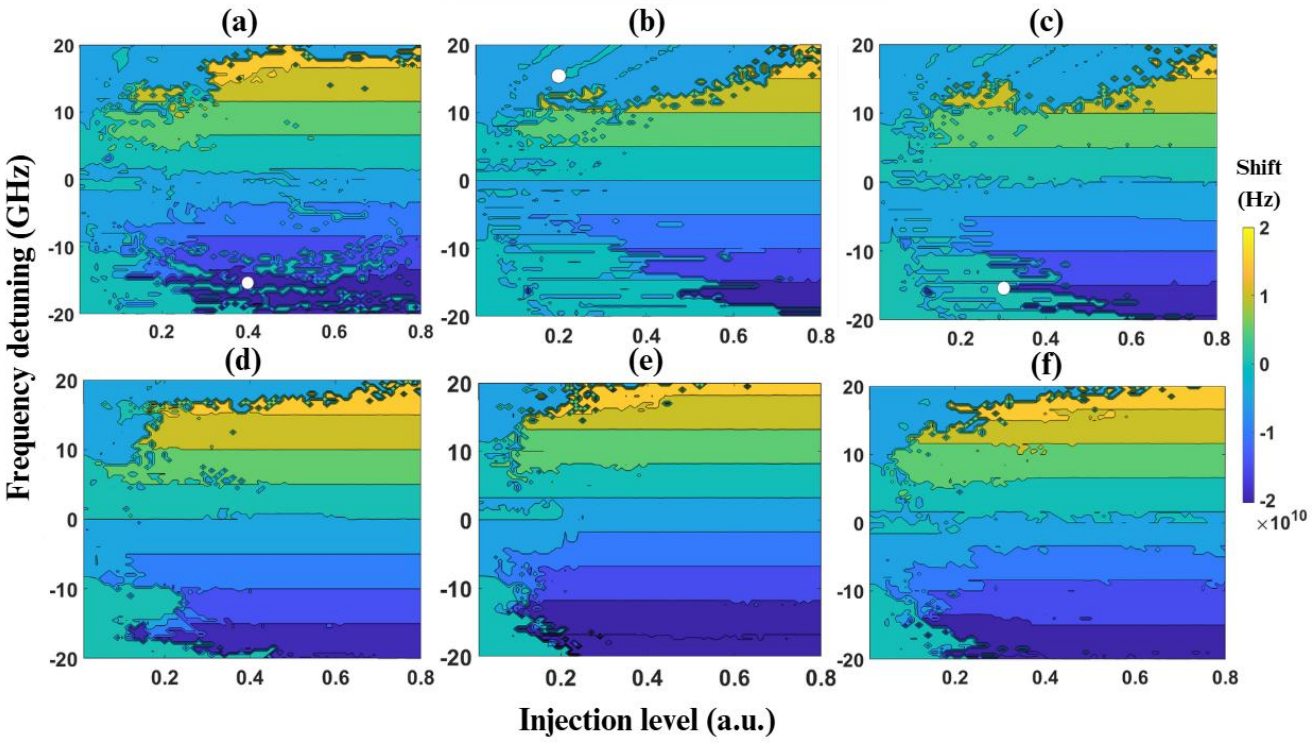

Fig. 4. Injection locking maps of the SL under the injection of: (a) normal, (b) Gaussian, (c) Lorentzian, (d) graded, (e) quadratic and (f) zigzag comb. The spacing in this case is 0.8 GHz and the color bar in the right illustrates the shift in the free-running SL peak. The white circles in (a), (b) and (c) represent the operating points at which the spectra in Fig. 5 are taken, respectively (colour online)

One of the most evident changes is the effect of increased frequency spacing on the locking regions. In Fig.

4, where the frequency spacing is 0.8 GHz, the locking regions are generally broader across most comb types compared to Fig. 2. This broadening suggests that larger frequency spacing facilitates wider regions of injection locking, enabling the SL to maintain locked states over a broader range of detuning values at a given injection level. However, while the locking range increases, there is also a tendency for the regions to become more fragmented, indicating a trade-off between breadth and stability in the locking behavior.

Examining individual comb types provides further insights into how increased spacing influences stability. For the normal comb, both Figs. display well-defined locking regions at mid-range detuning and injection levels. However, in Fig. 4, the locking region is slightly more dispersed, hinting at a broader but potentially less stable locking range due to the increased spacing. Gaussian and Lorentzian combs, which concentrate power around the central frequency, maintain narrow locking regions in both figures. Yet, the locking regions in Fig. 4 are somewhat less continuous, with more intermittent patches, especially noticeable in the Lorentzian comb. This fragmentation indicates that the larger frequency spacing reduces the smoothness of transitions, making the boundaries less stable.

The graded comb continues to exhibit smooth locking regions, although the increased spacing in Fig. 4 introduces some fragmented boundaries compared to the smoother transitions seen in Fig. 2. For quadratic and zigzag combs, the larger spacing brings out more complexity in their already fragmented locking regions. In Fig. 4, these combs display reduced stability at higher injection levels, with even more pronounced fragmentation. The zigzag comb shows a significant decrease in locking regions, demonstrating the destabilizing effect of increased frequency spacing on combs with alternating power distributions.

Intermittency and chaotic boundaries are also more pronounced in Fig. 4, especially along the upper locking boundary. The presence of dots along these boundaries, indicating partial locking or transitions to chaotic behavior, is more noticeable across all comb types in Fig. 4. The Lorentzian comb still shows the highest level of intermittency, with an even more unstable boundary due to the sharper power distribution decay. The quadratic and zigzag combs, which displayed the least intermittency in Fig. 2, now exhibit slightly more chaotic transitions, particularly at higher injection levels. However, they still retain relatively lower intermittency compared to Gaussian and Lorentzian combs, suggesting that despite the larger frequency spacing, these combs maintain some degree of stability near the chaotic boundary.

Therefore, increasing the frequency spacing from 0.2 GHz to 0.8 GHz results in broader locking regions but introduces more fragmentation and intermittency, especially along the boundaries. Gaussian and Lorentzian combs remain effective in creating predictable locking regions, though they show heightened instability at the edges. Quadratic and zigzag combs, while exhibiting more fragmentation with the larger spacing, continue to show reduced intermittency and relatively stable behavior near the chaotic boundary. This comparison highlights the complex interplay between frequency spacing and stability in injection-locked SL systems, demonstrating that while larger spacing can enhance the locking range, it may also induce more chaotic behavior at high detuning and injection levels.

Finally, one could conclude that the type of frequency comb injected into the slave laser (SL) consistently impacts its locking behavior, regardless of spacing. Normal combs create well-defined, locking regions at mid-range detuning, while Gaussian and Lorentzian combs, with concentrated central power, produce narrow, locking regions. The Gaussian comb's gradual decay allows smoother transitions, whereas the Lorentzian's sharp decay leads to higher intermittency. Graded combs offer better locking due to smooth power reduction. In contrast, quadratic and zigzag combs, with uneven power distributions, cause fragmented locking patterns but exhibit stable boundaries with reduced intermittency. Overall, Gaussian and Lorentzian combs yield predictable locking, whereas quadratic and zigzag combs show more complex but stable boundaries.

As for the optical spectra, the SL shows almost the same characteristics of locking and frequency pushing as shown in Fig. 5. In Fig. 5 a, the SL is locked to the ML comb at -15 GHz with an injection level of 0.4. The frequency pushing behavior is shown in Fig. 5 b and c, as the ML comb is injected outside the locking region. The only difference in this case (0.8 GHz spacing), is the enhancement of four-wave mixing FWM side peaks and periodicity as clearly shown in the spectra.

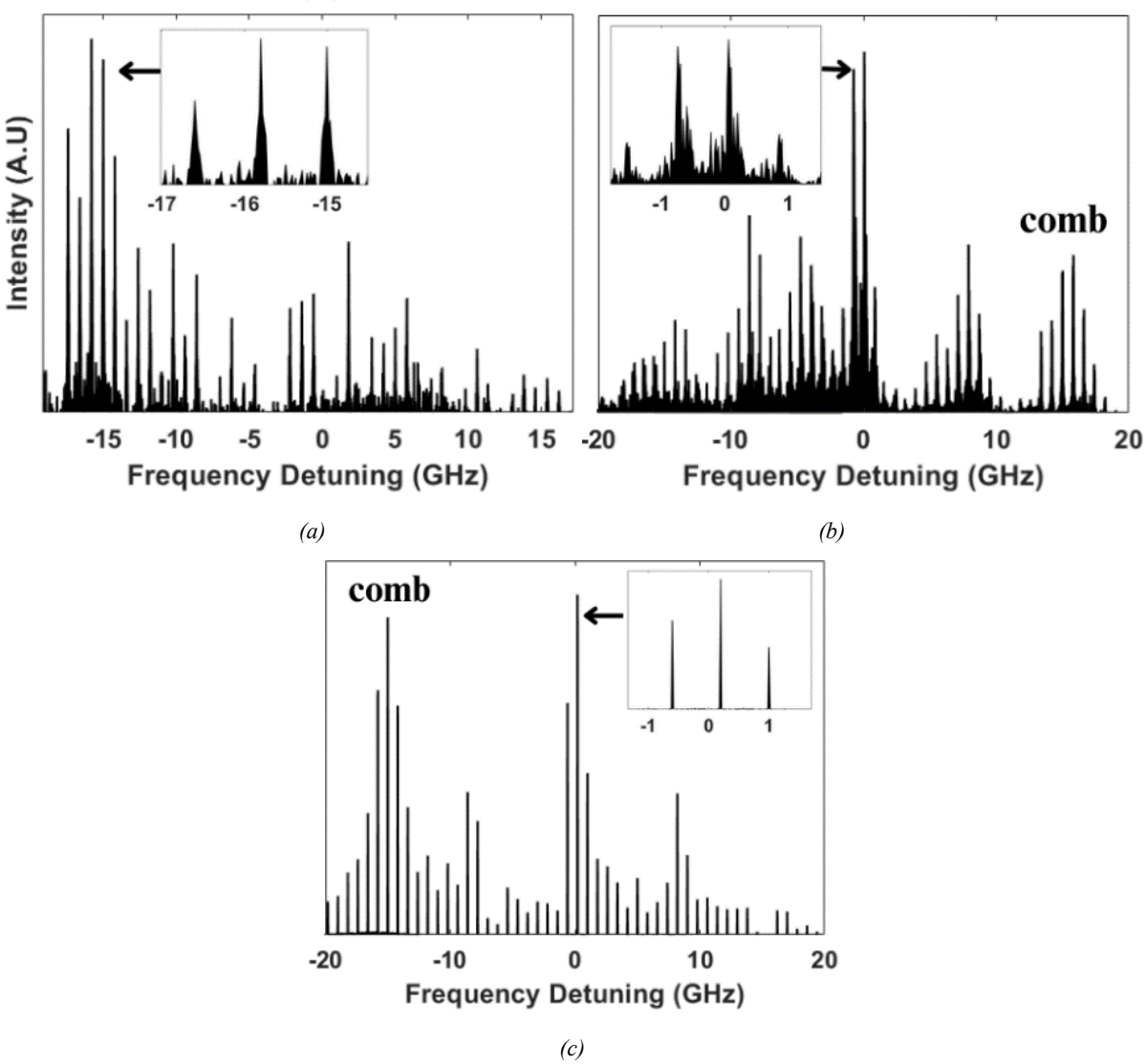

Fig. 5. Optical spectra of the injected SL (linear scale) at the points shown in Fig. 4 a, b and c, respectively. The insets are magnification of the indicated areas by arrows

For further inspection of the effect of comb type on the dynamics of the injected semiconductor lasers, we generate bifurcation diagrams of the system as a function of frequency detuning at a constant injection level of 0.1 as shown in Fig. 6. These diagrams highlight how each comb's unique power distribution affects the SL s dynamic response, including stability, periodicity, and chaotic dynamics. Notably, the bifurcation patterns vary among the six types of combs, indicating that each type of comb responds differently to detuning adjustments. One could see that the SL dynamics have less instabilities in the cases of Gaussian and Lorentzian comb injection (less density of dots) as shown in Fig. 6 b and c, respectively. However, the injection of Graded comb shows a very clear manner as shown in in Fig. 6 d, which displays a relatively more organized bifurcation pattern, potentially representing a more stable or predictable response to detuning. The rest of the comb types (Fig. 6 a, e and f) show a dense interweaving of extrema across detuning values, suggesting highly intricate bifurcation behaviors, likely indicative of chaotic or multi-stable regimes.

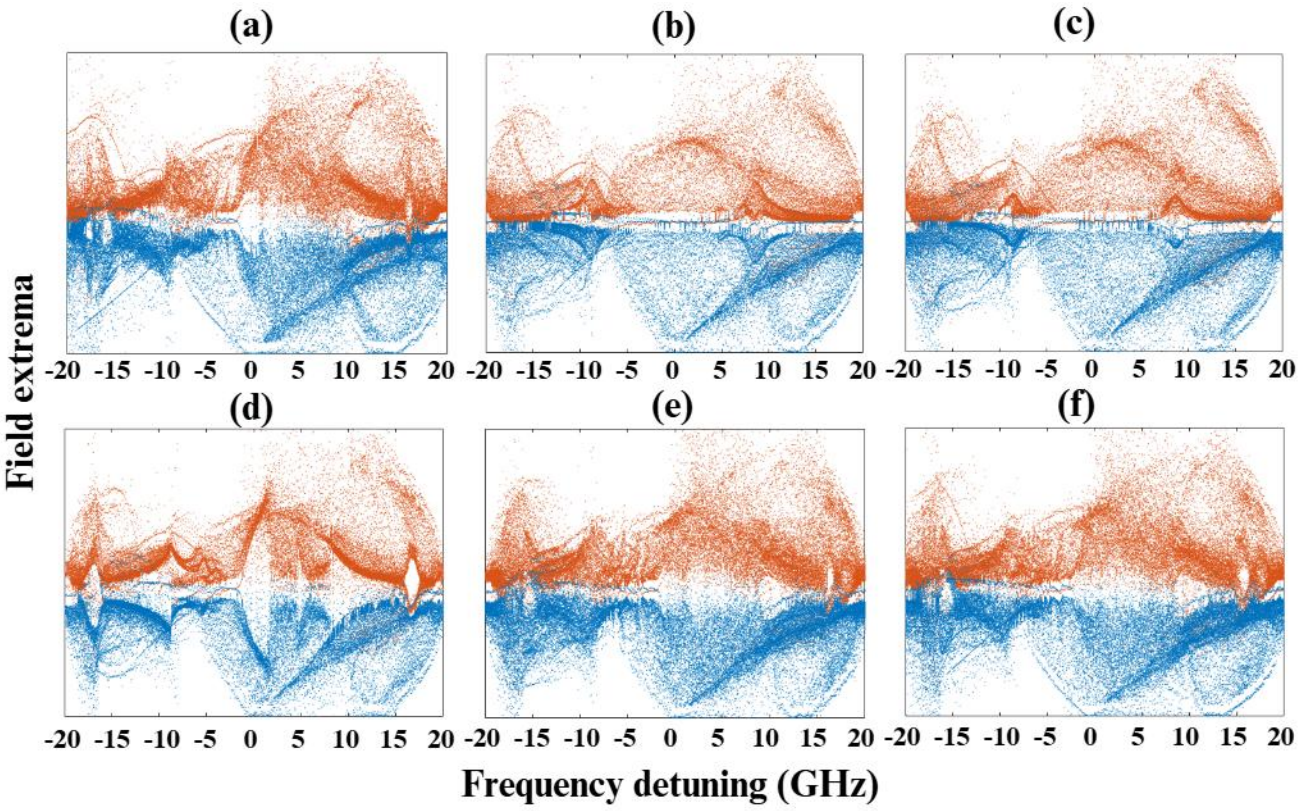

Fig. 6. Bifurcation diagrams of the same maps shown in Fig. 2 for the six types of combs. The field extrema are recorded as function of frequency detuning at constant injection level = 0.1. The two colors represent the two extrema (colour online)

Furthermore, Fig. 7 provides supporting evidence for these bifurcation patterns by detailing the relationship between the electric field and population inversion at the same detuning levels, highlighting how each comb's structure influences the internal population-field dynamics of the SL. At lower detuning values (e.g., -20 GHz), the phase portraits show simple, closed loops, indicating periodic behavior and a relatively stable, non-chaotic state. This simplicity reflects the more regular bifurcation structures observed in the earlier bifurcation diagrams at similar detuning values. As detuning approaches zero and then moves into positive values, the phase portraits become increasingly complex, with multiple loops and denser regions in phase space. This shift indicates a transition from regular periodicity to quasi-periodic or chaotic dynamics, aligning with the intricate bifurcation patterns observed in the previous figure at these detuning ranges. The patterns within each comb type differ in response to detuning, with some types (like Quadratic and Zigzag) showing more pronounced transitions to complex dynamics at specific detuning values compared to others. This divergence in behavior emphasizes that each comb type has a unique dynamic profile and responds differently to frequency detuning, which is critical for tuning comb characteristics in practical applications.

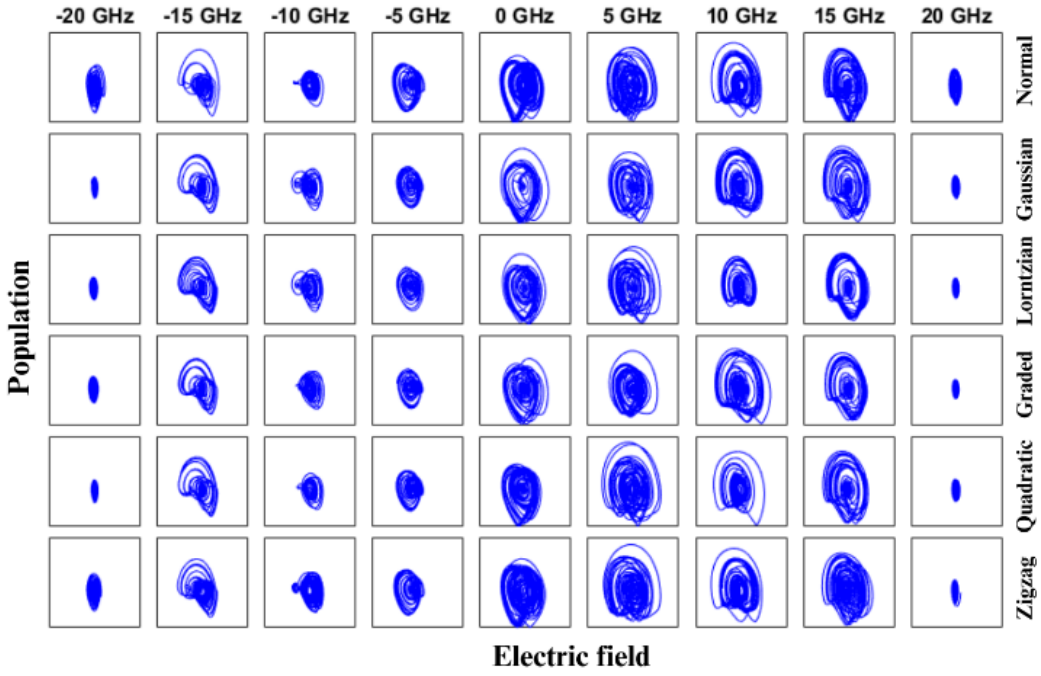

Fig. 7. Electric field vs population at different frequency detuning for the six types of combs. All points are taken at injection level 0.1, i.e. taken from Fig. 6 (colour online)

We have also generated the bifurcation diagrams as a function of injection levels as shown in Fig. 8, for each comb type, normal, Gaussian, Lorentzian, graded, quadratic, and zigzag, while maintaining a constant frequency detuning of -15 GHz. These diagrams provide an apparent view of how each comb profile affects the stability and dynamic behavior of the semiconductor laser, particularly in terms of transitions between periodic and chaotic states. The red and blue points in each panel again represent the two extrema of the oscillatory behavior, indicating peaks of the SL's field intensity over time, which can reveal the stability of the system under different injection conditions.

The normal comb profile, shown in Panel (a), exhibits a mix of stable and chaotic behavior as the injection level increases. At very low injection levels, the pattern is periodic, with clear, structured extrema, indicating stable oscillations. However, as the injection level rises, the system begins to transition into chaotic dynamics, with more scattered extrema points suggesting irregular oscillations. This gradual shift into chaotic behavior at higher injection levels indicates that the normal comb offers versatility but can lead to instability under strong injection, making it more suitable for applications that can tolerate or exploit such transitions.

The Gaussian comb, shown in panel (b), begins similarly with stable periodic behavior at low injection levels. However, it transitions into chaos more rapidly than the normal comb. The onset of chaotic dynamics occurs at slightly a lower injection threshold, as indicated by the scattered pattern of extrema points even at moderate injection levels. This higher sensitivity to changes in injection suggests that the Gaussian comb profile may be advantageous for applications that require fine-tuned control over laser modulation but could present challenges in scenarios where high stability is essential.

In panel (c), the Lorentzian comb displays a dynamic pattern very comparable to the Gaussian comb. The chaotic regions are prominent and widely dispersed across the injection level range, reflecting heightened sensitivity to small injection level changes and a rapid loss of periodicity. Moreover, the periodicity is more evident at high injection level than the case of Gaussian comb.

In contrast, the graded comb, depicted in panel (d), exhibits a markedly different behavior. It maintains a high degree of periodicity and stability across a wider range of injection levels compared to the Gaussian and Lorentzian combs. The bifurcation diagram shows fewer scattered points and a more organized pattern of extrema, indicating that the graded profile supports a stable response with limited chaotic regions, especially at very high injection levels. This stability suggests that the graded comb is well-suited for applications requiring consistent and predictable output, such as those in metrology or other precision-dependent fields.

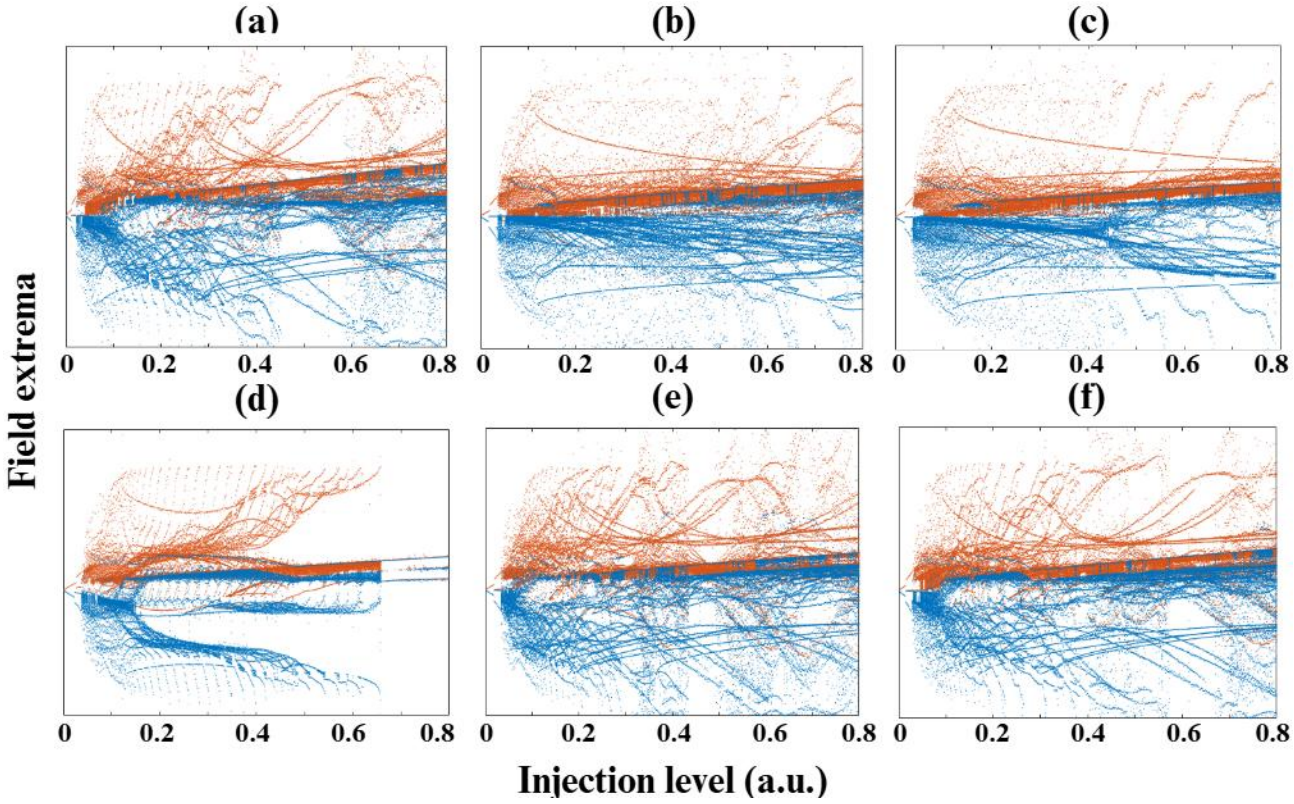

Fig. 8. Bifurcation diagrams of the same maps shown in Fig. 2. The field extrema are recorded as function of injection level and at a constant frequency detuning of -15 GHz. The two colors represent the two extrema (colour online)

The last two panels (e) and (f), shows the dynamics with the quadratic comb and zigzag comb, respectively. Both dynamics look almost similar. However, the dynamic in the case of quadratic comb (Fig. 8 f) displays stable and periodic behavior across most of the injection levels, with some evidence of chaotic regions. The well-defined extrema indicate that the SL maintains a periodic response, showing that the quadratic comb is ideal for applications where a stable and highly predictable laser output is critical. In contrast, the dynamic of the zigzag comb in Panel (f), presents a bifurcation structure that blends stability with occasional chaotic regions. At low injection levels, the response is stable and periodic, but as the injection level increases, small chaotic regions start to emerge. However, these chaotic regions are less pronounced compared to those of the Gaussian or Lorentzian combs. The zigzag profile's moderate sensitivity to changes in injection levels provides a balance between stability and complexity, potentially making it useful for applications that require flexible yet not overly chaotic behavior.

In summary, the bifurcation diagrams of Fig. 8 reveal that the normal, Gaussian, and Lorentzian combs tend to induce chaotic dynamics more readily as injection levels increase, with the Gaussian and Lorentzian profiles being especially sensitive to shifts in injection. In contrast, the graded, quadratic, and zigzag combs show greater stability, with fewer chaotic regions and more defined periodic behavior. Among these, the graded profile maintain stability across a broader range of injection levels, making it preferable for applications that require consistent and predictable laser behavior. The Gaussian and Lorentzian combs, which quickly transition to chaotic dynamics, may be better suited for applications that can benefit from or control chaotic outputs. The zigzag comb provides an intermediate behavior, allowing a balance between stability and controlled complexity, which could be valuable for applications where flexibility in response is desired without a complete loss of periodicity.

To support the previously mentioned conclusion, we have depicted the electric field versus population at different injection levels for the six types of combs as shown in Fig. 9. All points are taken at a frequency detuning of -15 GHz, corresponding to the conditions in Fig. 8. The patterns in Fig. 9 align with the bifurcation diagrams of Fig. 8, further illustrating how population dynamics evolve as injection levels increase across the six comb profiles. The normal comb shows smooth and symmetric contours at low injection levels, which transition into more scattered, chaotic structures as the injection level rises, mirroring the gradual onset of chaotic behavior seen in Fig. 8. The Gaussian comb rapidly loses periodicity with injection level increases, as evidenced by irregular and fragmented population contours even at moderate injection levels, which corresponds to its early transition into chaos in the

bifurcation diagram. The Lorentzian comb, characterized by heightened chaotic regions in Fig. 8, exhibits significantly fragmented and irregular contours in Fig. 9, reflecting its nonlinear sensitivity to higher injection levels.

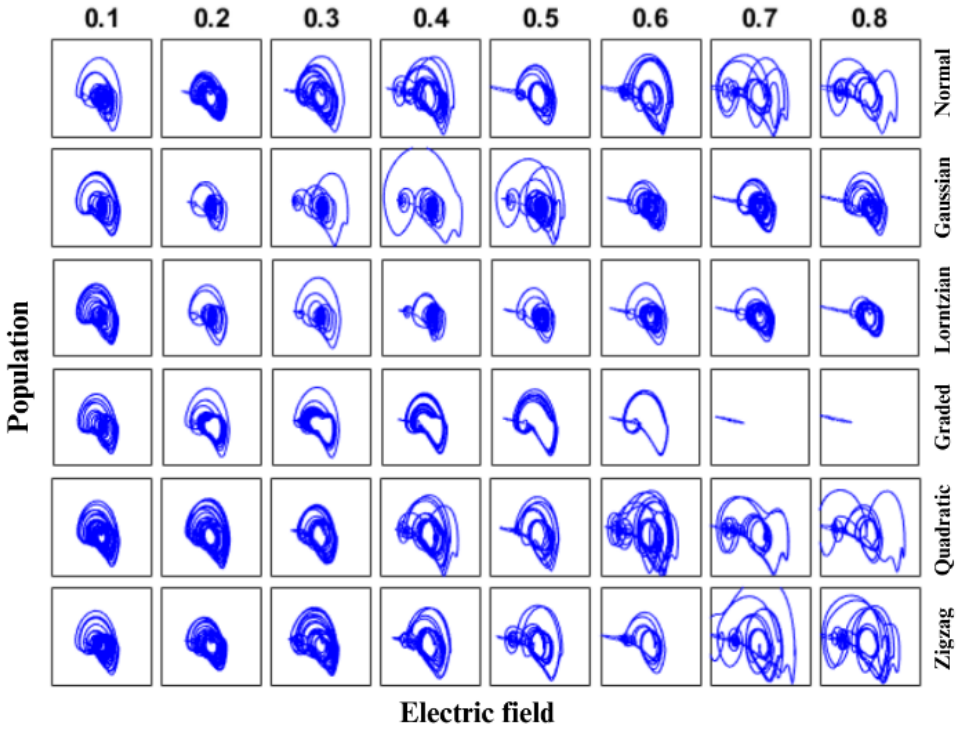

Fig. 9. Electric field vs population at different injection levels for the six types of combs. All points are taken at frequency detuning of -15 GHz, i.e. taken from Fig. 8 (colour online)

In contrast, the graded comb demonstrates stable, well-organized population dynamics across all injection levels, consistent with its extended stability shown in Fig. 8. Similarly, the quadratic comb maintains distinct and regular population contours, reinforcing its periodic and predictable behavior noted previously. The zigzag comb, while stable at low injection levels, begins to display moderate irregularities as the injection level increases, but these chaotic regions are less pronounced than those of the Gaussian or Lorentzian combs, reflecting its intermediate stability described in Fig. 8. Together, Fig. 9 supports the conclusion that comb profiles like graded and quadratic ensure stable and predictable laser dynamics, while Gaussian and Lorentzian profiles introduce more chaos, providing flexibility for applications requiring tunable complexity.

Finally, we have investigated the dynamics of carrier's density as a function of frequency detuning for the six types of combs at a constant injection level of 0.1 and frequency spacing of 0.2 GHz and 0.8 GHz, as shown in Fig. 10 a and b, respectively. The general characteristic of the carrier dynamics reported before [29] is evident here in both cases, including, the asymmetry around 0 GHz and the depletion of carrier in the negative detuning side. However, insight look at the dynamics of carriers in the case of 0.2 GHz spacing (left graph in Fig. 10) reveals that the type of the injected comb can largely affect the dynamics of carriers especially in the negative detuning side. For example, normal and zigzag combs (black and purple curves) illustrate enhanced carrier density in this region (negative detuning side), while the rest of comb types show no differences. The gradient of the curves near 0 GHz detuning represents the locking bandwidth and the distinct locking regions of the Gaussian and Lorentzian (red and green curves) are evident. In the positive detuning side, all comb types show almost the same dynamics as shown in the figure. For the case of 0.8 GHz spacing (right graph in Fig. 10), the enhancement of periodicity and chaos results in large fluctuation in carrier dynamics and hence making them undistinguishable, with the normal and zigzag combs having the largest observed fluctuation among all the comb types. The investigation of carrier dynamics is particularly important as these dynamics were found to be the responsible effect behind the observed frequency shift in optically injected semiconductor lasers [29]. In other words, comb type can be used as an effective tool to tailor frequency shift observed outside the locking bandwidth.

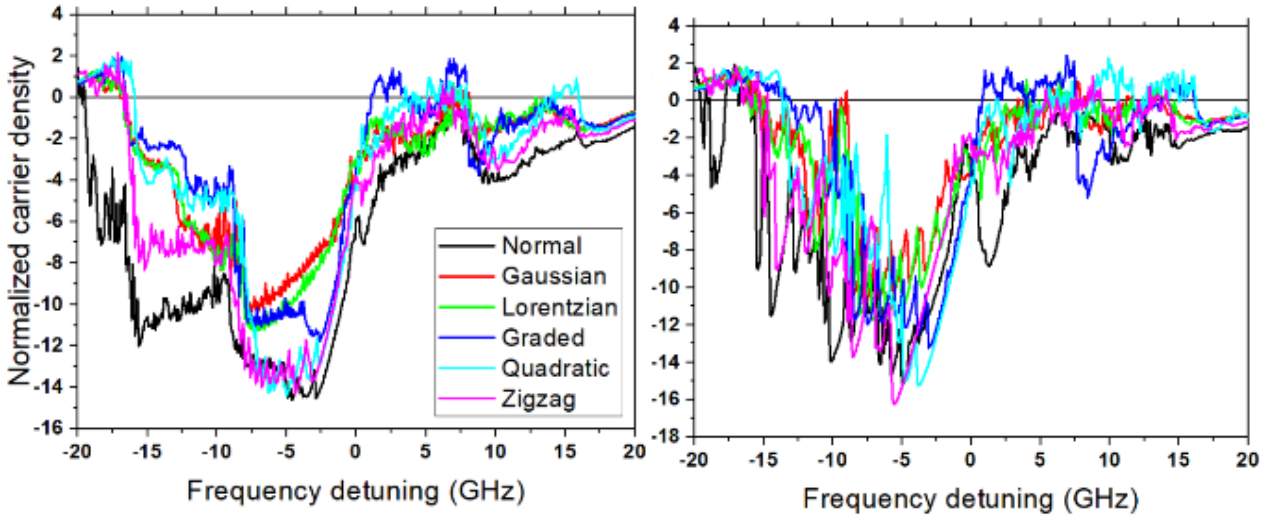

Fig. 10. Carriers' density variation as a function of frequency detuning for the six types of combs at a constant injection level of 0.1 and frequency spacing of 0.2 GHz (left) and 0.8 GHz (right) (colour online)

The relaxation oscillation frequency (ROF) of the slave laser, estimated using $G_N=1.4\times10^{-12}$ m^3/s, and $\tau_p=1.8$ ps, is approximately 8–10 GHz under our injection conditions (at $I/I_{th}=2$). Since the comb spacings investigated in this study (0.2 GHz and 0.8 GHz) are significantly lower, the dynamics observed occur well below the ROF. Therefore, no resonance effects between the comb and ROF were observed. Future studies may explore near-ROF operation to assess potential dynamic modulation or instabilities.

Noise is an inherent factor in optical systems and plays a significant role in the dynamics of frequency combs. Its presence can influence the stability of injection-locking, the predictability of locking boundaries, and the transition to chaotic regimes. In particular, amplitude and phase noise in the master laser can propagate through the injection process, impacting the comb's spectral purity and the slave laser's output stability.

Noise can also modulate the linewidth of the comb modes, potentially reduce the effective locking range and increase intermittency near chaotic boundaries. While the current study focuses on deterministic modeling, future work will incorporate noise effects to provide a more realistic representation of real-world systems. This will include simulating additive white Gaussian noise (AWGN) to model amplitude and phase fluctuations, as well as examining its impact on bifurcation behavior, intermittency, and carrier dynamics. Experimental validations will further quantify noise-induced variations, offering insights into optimizing the robustness of frequency comb-based systems under realistic conditions. It is worth noting that gain compression effects were not included in the present model. While this omission simplifies the rate equations, it may lead to overestimation of intensity modulation and chaotic dynamics at high injection levels. Including gain compression (e.g., via a saturation term in the gain coefficient) would likely reduce the amplitude of fluctuations and may slightly shift the boundaries of locking and chaotic regions. Future work will aim to incorporate this nonlinearity to refine the predictive accuracy of the model, particularly under strong optical injection.

4. Conclusions

This work highlights the significant influence of frequency comb profiles on the dynamic behavior of optically injected semiconductor lasers. Gaussian and Lorentzian combs provide smooth and predictable locking regions but are prone to instability near chaotic boundaries, especially with increased frequency spacing. In contrast, quadratic and zigzag combs demonstrate greater boundary stability despite their fragmented locking patterns. Graded combs emerge as a balance, delivering consistent and stable performance across injection and detuning variations. Our bifurcation and carrier dynamics analyses further emphasize the adaptability of comb characteristics in tuning laser dynamics, where stable responses or controlled chaotic behaviors are required. These insights contribute to advancing the design and optimization of frequency comb-based optical systems for applications ranging from metrology to advanced communication systems.

Acknowledgments

The authors would like to acknowledge the Deanship of Graduate Studies and Scientific Research, Taif University for funding this work.

References

[1] S. Kobayashi, T. Kimura, IEEE J. Quantum Electron. **17**, (681 (1981).
[2] F. Mogensen, H. Olesen, G. Jacobsen, IEEE J.

Quantum Electron. **21**, 784 (1985).
[3] Z. Liu, R. Slavík, J. Lightwave Technol. **38**, 43 (2020).
[4] A. Rosado, E. P. Martin, A. Perez-Serrano, J. M. G. Tijero, I. Esquivias, P. M. Anandarajah, Opt. Laser Technol. **131**, 106392 (2020).
[5] E. Sooudi, S. Sygletos, A. D. Ellis, G. Huyet, J. G. McInerney, F. Lelarge, Kamel Merghem, Ricardo Rosales, Anthony Martinez, Abderrahim Ramdane, Stephen P. Hegarty, IEEE J. Quantum Electron. **48**, 1327 (2012).
[6] H.-T. Tang, Y.-H. Hung, Opt. Lett. **48**, 6436 (2023).
[7] H. M. Hussein, S. Kim, M. Rinaldi, A. Alù, C. Cassella, Nat. Commun. **15**, 2844 (2024).
[8] N. M. Al-Hosiny, I. D. Henning, M. J. Adams, Opt. Commun. **269**, 166 (2007).
[9] Y. Doumbia, T. Malica, D. Wolfersberger, K. Panajotov, M. Sciamanna, Opt. Lett. **45**, 435 (2020).
[10] Y. Doumbia, T. Malica, D. Wolfersberger, M. Sciamanna, Opt. Lett. **48**, 1442 (2023).
[11] A. Borodkin, A. Kovalev, M. Giudici, G. Huyet, A. Ramdane, M. Marconi, E.A. Viktorov, Conference on Lasers and Electro-Optics/Europe (CLEO/Europe 2023) and European Quantum Electronics Conference (EQEC 2023).
[12] M. Al Mulla, Optik **223**, 165506 (2020).
[13] T. Ramond, L. Hollberg, P. Juodawlkis, S. Calawa, Appl. Phys. Lett. **90**, 181124 (2007).
[14] K.-P. Ho, J. M. Kahn, IEEE Photon. Technol. Lett. **5**, 721 (1993).
[15] X. Zhang, C. Wang, Z. Cheng, C. Hu, X. Ji, Y. Su, Nanophotonics **1**, 26 (2024).
[16] N. M. Al-Hosiny, I. D. Henning, M. J. Adams, IEEE J. Quantum Electron. **42**(6), 570 (2006).
[17] M. I. Khan, Z. Xiao, S. J. Addamane, D. Burghoff, Proc. SPIE **12869**, 1286901 (2024).
[18] A. Gavrielides, IEEE J. Quantum Electron. **50**, 364 (2014).
[19] H. Moon, E. Kim, S. Park, C. Park, Appl. Phys. Lett. **89**, 181108 (2006).
[20] K. Shortiss, B. Lingnau, F. Dubois, B. Kelleher, F. H. Peters, Opt. Express **27**, 36976 (2019).
[21] A. E. Ulanov, T. Wildi, N. G. Pavlov, J. D. Jost, M. Karpov, T. Herr, Nat. Photonics **18**, 294 (2024).
[22] T. Wildi, A. E. Ulanov, T. Voumard, B. Ruhnke, T. Herr, Nat. Commun. **15**, 7030 (2024).
[23] S. Wieczorek, B. Krauskopf, T. Simpson, D. Lenstra, Phys. Rep. **416**(1-2) 1 (2005).
[24] A. Stroganov, A. Kovalev, E. Viktorov, Phys. Rev. E **107**, 034208 (2023).
[25] V. Sharma, S. Singh, E. A. Anashkina, A. V. Andrianov, Optik **241**, 166948 (2021).
[26] Y. Doumbia, T. Malica, D. Wolfersberger, K. Panajotov, M. Sciamanna, Opt. Express **28**, 30379 (2020).
[27] X.-Z. Li, J.-P. Zhuang, S.-S. Li, J.-B. Gao, S.-C. Chan, Phys. Rev. E **94**, 042214 (2016).
[28] J. Ohtsubo, Semiconductor Lasers: Stability, Instability, and Chaos, Springer, 2017.
[29] N. M. Al-Hosiny, Photonics **9**, 886 (2022).
[30] W. Althobaity, S. Al Harthi, N. Al-Hosiny, Results Eng. **23**, 102812 (2024).

*Corresponding author: najm@tu.edu.sa